

## Effect of Microstructure on Mechanical Property of Carbon Steel/Strainless Steel Rolling Clad Plate

Li Hai-bin<sup>1,2</sup>, Zhou Cun-long<sup>3</sup>, Fan Xiao-ning<sup>3</sup>, Kong Yi-gang<sup>3</sup>, Huang Qing-xue<sup>2</sup>  
and Ma Qin<sup>1</sup>

<sup>1</sup>*School of Material Science and Engineering, Lanzhou University of Technology, Lanzhou 730050, China*

<sup>2</sup>*School of Material Science and Engineering, Taiyuan University of Science and Technology, Taiyuan, 030024, China*

<sup>3</sup>*College of Mechanical Engineering, Taiyuan University of Science and Technology, Taiyuan 030024, China*

*LI Hai-bin (1974- ), Male, Doctor, lecture  
<sup>a</sup>lihaibin19750300@sina.com,*

### Abstract

*The bonding interface microstructure and mechanical property of clad plate with different hot rolling schedules were researched. The results show that the carbide layer thickness of bonding interface increases firstly and then decreases with increasing reduction ratio. The carbide layer of bonding interface is the major factor relating to tensile strength, so the experimental values of clad plate are slightly higher than the calculated ones. Moreover, the bending strength of clad plate is mainly influenced by the thickness ratio and the carbide quantity of SS, while the carbide layer thickness of bonding interface is an important factor affects the bending strength.*

**Keywords:** hot rolling; clad plate; microstructure; mechanical property

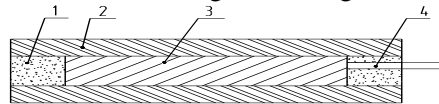
### 1. Introduction

Stainless steel (SS) /carbon steel (CS) clad plate refers to such a clad plate whose base layer is carbon steel, and clad layer is stainless steel. Two kinds of materials are bonded together by the special deformation process [1-2]. It is widely used in petroleum and chemical industry. Not only it has good toughness, corrosion resistance and beauty of the SS, but also has high strength and low-cost of CS. Hence there is a dramatically increasing demand of product in recent years [3]. The main fabricating method of clad plate is explosion-rolling method at present. However, it could not be carried out in large scale because of the restriction of production technology such as severe pollution, high cost and the limited size of the clad plate [4-6]. Moreover, a great deal of attention was paid on product quality defects such as the shrinkage cavity, crack, stomata of the bonding interface under explosive blast wave [7]. Hot-rolling bonding has the advantages of economical and efficient production capacity, less pollution and low energy consumption, which has attracted wider attention. However, the bonding rate, bonding quality and heat treatment process have some deficiencies under present production technology [8-9]. The interface is easy to be oxidized at high temperature, which incurs reduced strength of the clad interface. In order to effectively avoid oxidation, the vacuum hot rolling bonding (VHRB) has been applied [10-13]. Two kinds of steels were all-around welded that clad billets were obtained after vacuum pumping of the inner space. In addition, previous studies mostly concern on the microstructure of bonding interface, while the influence of microstructure on the mechanical property of clad plate has seldom been reported.

The base and the clad materials used in this study were carbon steel (Q235A) and austenitic stainless steel (304). The origin plate thickness was 5.5 mm for CS and 2.5 mm for SS. The main chemical compositions of the CS are C(0.1%), Mn(0.5%), Si(0.3%), S(0.050%), P(0.045%) and Fe(Bal.). The main chemical compositions of the SS were C(0.03%), Si(0.43%), Mn(1.21%), Cr(18.23%), Ni(8.03%) and Fe(Bal.). Microstructure evolution of the clad plate is observed by scanning electron microscope (SEM). Furthermore, the mechanical properties of clad steel plate were studied.

## 2. Materials and Methods

The specimen is composed of CS in the middle and SS on the outer surface. The entire specification of bonding billets was 15mm thick, 125mm wide and 150mm long. The diagram of the sample preparation is showed in Figure 1. The billets were heated to 1300°C in the heating furnace and were soaked for 15 minutes. This was immediately followed by one or two pass rolling on a two-high reversible rolling mill (with the roller diameter of 320 mm, roller width of 350mm) at the rolling speed of 0.1m/s. The pre/post-rolling upper surface temperature of the clad plate was examined using the TI300 and AR892 non-contact infrared temperature measurement instrument. Different rolling technologies are shown in Table 1.



1.welded seam 2.carbon steel 3.stainless steel 4. the pipe for vacuum-pumping

**Figure 1. Diagram of Experimental Sample Preparation**

**Table 1. Rolling Processes of Three Clad Plates**

No.	rolling force/T	pre/post-rolling temperature/°C		reduction rate/%
		pass 1	pass 2	
1#	41	1081/975	--	20
2#	66	1023/929	--	30
3#	63/72	1134/1028	888/783	30/20

## 3. Results

Figure 2 (a), (b), and (c) display the bonding interface microstructures of the sample 1, sample 2 and sample 3, respectively. Previous study shows only ferrite precipitated near the bonding interface [14] which is tens of micron wide from Figure 2 (a), where there were pro-eutectoid ferrite and ferrite with granular carbides. The carbide layer of bonding interface is about 3µm and SS is on the right of photograph. Figure 2 (b), shows all ferrite grains are with granular carbides near the bonding interface and the thickness of carbide layer slightly increases. As shown in Figure 2(c), the granular carbides are fine and its quantity is more than the former. However, the carbide layer thickness of bonding interface decreases.

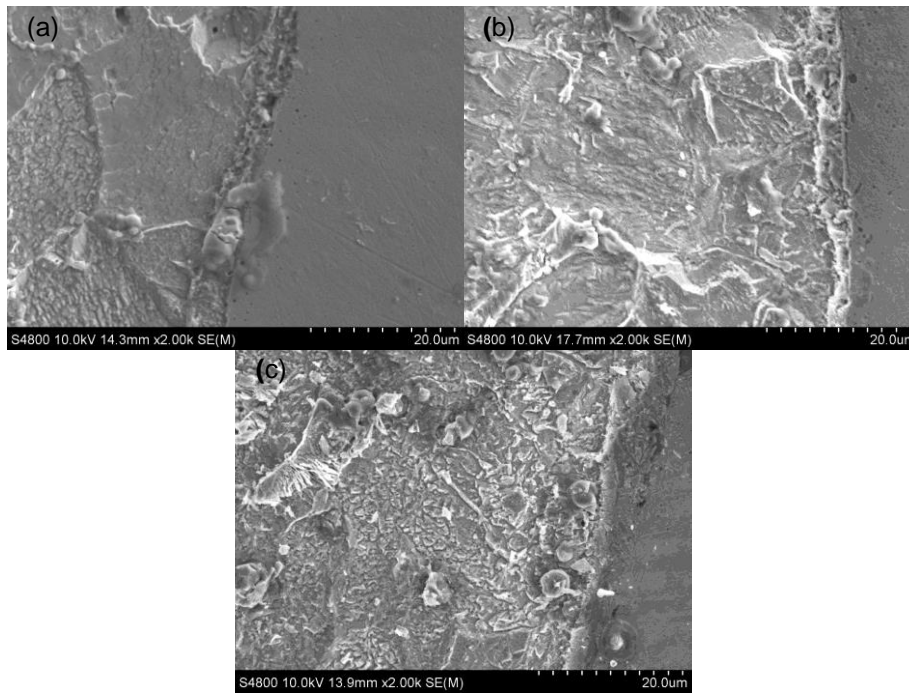


**Figure 2. Microstructure of Bonding Interface for Hot-Rolled Clad Plate (a) 1# (b)2# (c) 3#**

### 3.1. The Tensile Strength

The tensile test of the specimens is investigated. The tensile strength, the thickness of clad plate (D/mm), the thickness ratio of SS ( $\beta$ /%) are listed in Table 2. The elongation percentages ( $\delta$ /%) are calculated from Equation (1):

$$\delta = \frac{l - l_0}{l_0} \times \% = \frac{\Delta l}{l_0} \times \% \quad (1)$$

**Table 2. Calculate and Measured Values of Tensile Test**

No.	$\sigma_b$ /MPa	$\sigma_{CS}$ /MPa	$\sigma_{SS}$ /MPa	D/mm	$\beta$ /%	$\delta$ /%
1#	498.8	438.8	521.3	8.6	55.0	76.2
2#	529.7	473.3	556.2	7.0	37.6	78.8
3#	586.6	533.1	623.2	5.8	28.7	80.3

The experimental results show that the tensile strength increases with increasing reduction ratio. The specimen is composed of SS(upper and lower layer) and its thickness is about one half of the clad plate, while the thickness ratio of SS decreases with reduction ratio increases, which indicate that the soft SS at high temperature deform easily than CS and the tensile strength of clad plate mainly provided by CS. Furthermore, the carbon atom diffuses under the action of rolling interior stress, and the grain size of CS and SS decreases with reduction ratio increases [14-15], the precipitated carbides are fine and uniform. The tensile strength increase because the fine grain retards the migration of grain boundaries for the pinning effect.

The CS fracture morphology of sample 2<sup>#</sup> and 3<sup>#</sup> are shown in Figure 3(a), and (b). The fractograph of Figure 3(a), shows that uniform dimples distribute on the fracture and there is a carbide particle in each dimple with different sizes. A few carbides show evident characteristic of intergranular brittle rupture. However, the dimples in the fracture have different sizes, and many smaller dimples gather where there are no carbide particles from Figure 3(b). The dimples is deeper than the former. The results show carbon atom of CS distributes evenly when the reduction ratio is 44%, so that the specimen has been stressed uniformly and the stress concentration was reduced, which makes the carrying capacity of matrix increasing.

Figure 4(a), and (b) are the SS fracture morphology of sample 2<sup>#</sup> and 3<sup>#</sup>. The fractograph of SS covered with fine equiaxed dimples from Figure 4(a), which are shallow and the diameters are about 1μm. A few small pieces of SS are attached to the fractograph surface. It can be seen from Figure 4(b), that the size of dimples are slightly larger and the deepness of dimples increases, where there are not small pieces on the surface and it is fully plastic failure. The elongation percentage can reach 80.3%.

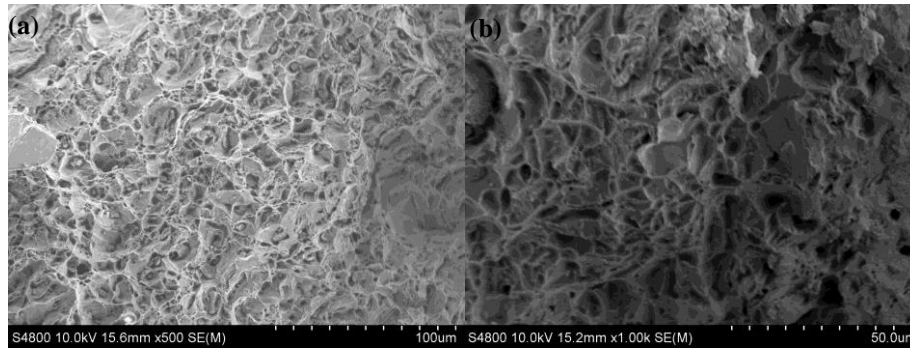


**Figure 3. Fractography of CS with Different Reduction Ratios (a) 2<sup>#</sup>  
 (b) 3<sup>#</sup>**

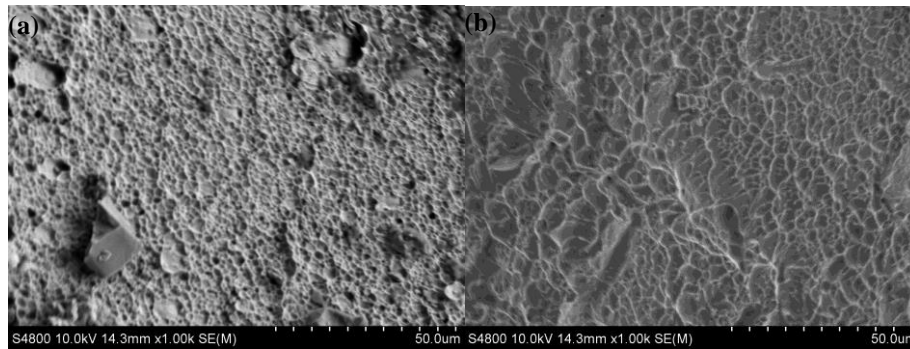


**Figure 4. Fractography of SS with Different Reduction Ratios (a) 2<sup>#</sup>  
 (b) 3<sup>#</sup>**

### 3.2. Difference between Experimental and Calculated Values

Detached the SS/CS bonding interface of samples using a special method, the tensile test of CS and SS is investigated, respectively, the results are shown in Table 2. The tensile strength could be described accurately by the equation:

$$R_m = \frac{t_{cs}\sigma_{cs} - t_{ss}\sigma_{ss}}{t_{cs} + t_{ss}} \quad (2)$$

Where  $\sigma_{SS}$  is the tensile strength of clad material,  $\sigma_{CS}$  is the tensile strength of base material,  $t_{SS}$  is the thickness of clad material,  $t_{CS}$  is the thickness of base material.

The calculated values of tensile strength are slightly lower than the experimental values from Figure 5. The results show that the tensile strength of the clad plate isn't only simple tensile strength combination of the two materials, the carbide layer of bonding interface is the major factor relating to the tensile strength. The measured tensile strength of clad plate is higher than the calculated one due to the existence of carbide layer. The difference between experimental and calculated values increases with thickness of carbide layer increasing, while there is less difference for specimen 3 in which there is no carbide layer.

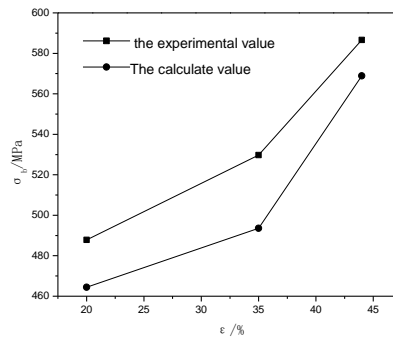


**Figure 5. Experimental and Calculate Values of Tensile Strength**

### 3. 3. Bending Strength

The bending strength of CS/SS clad plate is investigated by the 3-point bend loading method from the international standard of GB/T 232. The bending angle is 120° and the loading speeds is  $5.0 \times 10^{-4}$  m/s, the bending strength is calculated from the equation:

$$\sigma_f = \frac{3FL}{2bh^2} \quad (3)$$

**Table 3. Bending Strength of Clad Plates**

No.	1#	2#	3#
bending strength/MPa	653	802	636
H <sub>VSS</sub>	219.6	251.8	243.2
H <sub>VCS</sub>	142.2	162.2	171.8
H <sub>VI</sub>	189.1	195.4	228.7

The results are showed in Table 3. The bending strength increases firstly and then decreases with increasing reduction ratio. The grain size decreases with increasing reduction ratio and it is closely related to the tensile strength, but it does not obvious affect the bending strength. Furthermore, the bending strength of sample 3# is lowest as CS is the thickest, it is obvious to indicate that bending strength is mainly contributed from SS with high hardness.

The microhardness of original specimen had been tested by HDX-1000 type micro-Vickers sclerometer, the values are listed in Table 2. The microhardness of CS (H<sub>VCS</sub>) is lower than the carbide of bonding interface (H<sub>VI</sub>), and SS has the highest hardness (H<sub>VSS</sub>). The tensile strength is proportional to the hardness, hence the tensile strength of clad plate with the hard carbide layer is higher than the calculated values.

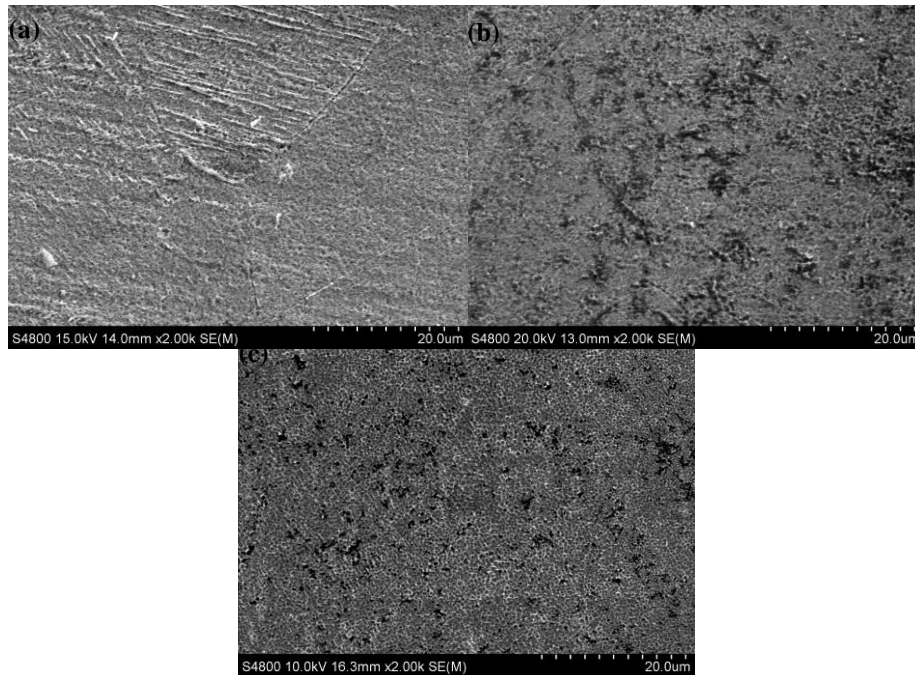


**Figure 6. Microstructure of SS by Hot-Rolling Clad Plate (a) 1# (b)2# (c) 3#**

SS microstructures of sample 1#, 2# and 3# are shown in Figure 6, respectively. The microstructure of SS is composed of austenite grain where some carbide strips precipitate from Figure 6(a). When reduction ratio is 30%, the quantity of carbide increases and it becomes carbide particles in Figure 6(b). The amount of high hardness carbide is more than the former, and it is proportional to the bending strength, although the thickness ratio of SS decreases. However, the bending strength of sample 3# decreases with reduction ratio increasing because of the carbide of SS is almost disappear from Figure 6(c), and the thickness ratio of SS is the lowest of all. Moreover, the high-hardness carbide layer of bonding interface is important to the bending strength.

#### **4. Conclusion**

(1) The carbide layer thickness of bonding interface increases firstly and then decreases with reduction ratio increases. The grain size of matrix decreases with reduction ratio increases that is an important factor to improve the tensile strength.

(2) The experimental values of tensile strength are slightly higher than the calculated ones due to the clad plate with carbide layer of bonding interface.

(3) The bending strength of clad plate is mainly influenced by the thickness ratio and the carbide of SS, while the carbide layer of bonding interface is an important factor to bending strength.

#### **Acknowledgments**

This work was financially supported by the National Basic Research Program of China ((2012CB722801), National Natural Science Foundation of China (51404159), Taiyuan University of Science & Technology Doctoral Fund (No.20122029) and National Natural Science Foundation of China (Grant No. 51275329).

## References

- [1] Y. M. Hwang and G. Y. Tzou, *Journal of Mater. Process. Tech.*, vol. 62, (1996).
- [2] Q. X. Huang, X. R. Yang and L. F. Ma, *Journal of Iron. Steel. Res. Int.*, vol. 21, (2014).
- [3] S. C. Pan, M. N. Huang and G. Y. Tzou, *Journal of Mater. Process. Tech.*, vol. 177, (2006).
- [4] HZheng, X. N. Ye, J. D. Li, *Mater. Sci. Eng., A.*, vol. 527, (2010).
- [5] P. Wang, S. P. Lu, N. M. Xiao, *Mater. Sci. Eng., A.*, vol. 527, (2010).
- [6] C. Jeong, T. Oya and J. Yanagimoto, *Journal of Mater. Process. Tech.*, vol. 213, (2013).
- [7] Z. G. Luo, G. M. Xie, G. L. Wang, *Chin. Journal of Mater. Res.*, vol. 27, (2013).
- [8] M. M. Sun, Z. Y. Chen and Y. Y. Bu, *Corros. Sci.*, vol. 82, (2014).
- [9] K. Bulent and Ç. Adnan, *Mater Charact.*, vol. 60, (2009).
- [10] A. H. Heuer, F. Ernst, Kahn H. *Scripta Mater.*, vol 56, (2007).
- [11] K. Yilamu, R. Hino and H. Hamasaki, *Journal of Mater. Process. Tech.*, vol. 210, (2010).
- [12] S. T. Hong, W. Kim and Y. J. You, *Trans. Nonferrous Met. Soc. China*, vol. 19, (2009).
- [13] K. Takuya and S. Akio, *Procedia Engineering*, vol. 81, (2014).
- [14] H. B. LI, Q. X. Huang and C. L. Zhou, *T Mater Heat Treat.*, vol. 35, (2014).
- [15] Q. X. Huang, H. B. Li, C. L. Zhou, *T Mater Heat Treat.*, vol. 35, (2014).

## Author



**Li Hai-bin**, Address correspondence to this author at the College of Material Science and Engineering, Taiyuan University of Science and Technology, 030024, P.R. China; Tel: +8613633473659; e-mail:lihaibin19750300@sina.com

